Title

Efficient Synthesis of Heparinoid Bioconjugates for Tailoring FGF2 Activity at the Stem Cell–Matrix Interface

Journal

Bioconjugate Chemistry, 30(3)

ISSN

1043-1802

Authors

Trieger, Greg W
Verespy, Stephen
Gordts, Philip LSM
et al.

Publication Date

2019-03-20

DOI

10.1021/acs.bioconjchem.8b00921

Peer reviewed

HHS Public Access

Author manuscript

Bioconjug Chem. Author manuscript; available in PMC 2019 November 18.

Published in final edited form as:

Bioconjug Chem. 2019 March 20; 30(3): 833–840. doi:10.1021/acs.bioconjchem.8b00921.

Efficient Synthesis of Heparinoid Bioconjugates for Tailoring FGF2 Activity at the Stem Cell–Matrix Interface

Greg W. Trieger[†], **Stephen Verespy III**[†,#], **Philip L. S. M. Gordts**[‡,§], **Kamil Godula**[*,†,§]

[†]Department of Chemistry and Biochemistry, University of California San Diego, 9500 Gilman Drive, La Jolla, California 92093-0358, United States

[‡]Department of Medicine, Division of Endocrinology and Metabolism, University of California San Diego, 9500 Gilman Drive, La Jolla California 92093-0687, United States

[§]Glycobiology Research and Training Center, University of California San Diego, 9500 Gilman Drive, La Jolla California 92093-0687, United States

Abstract

Heparan sulfate glycosaminoglycans (HS GAGs) attached to proteoglycans harbor high affinity binding sites for various growth factors (GFs) and direct their organization and activity across the cell–matrix interface. Here, we describe a mild and efficient method for generating HS–protein conjugates. The two-step process utilizes a “copper-free click” coupling between differentially sulfated heparinoids primed at their reducing end with an azide handle and a bovine serum albumin protein modified with complementary cyclooctyne functionality. When adsorbed on tissue culture substrates, the glycoconjugates served as extracellular matrix proteoglycan models with the ability to sequester FGF2 and influence mesenchymal stem cell proliferation based on the structure of their HS GAG component.

Graphical Abstract

[*]**Corresponding Author:** kgodula@ucsd.edu.

[#]**Present Address:** Encodia, Inc. 11125 Flintkote Ave., Suite B, San Diego, CA 92121

Author Contributions

The manuscript was written through contributions of all authors. All authors have given approval to the final version of the manuscript.

Supporting Information

The Supporting Information is available free of charge on the ACS Publications website at DOI: 10.1021/acs.bioconjchem.8b00921. Detailed experimental procedures and methods, spectral and chromatographic characterization, and extended biochemical and biological characterization of heparin- and heparinoid conjugates, and a complete list of Abbreviations (PDF)

The authors declare no competing financial interest.

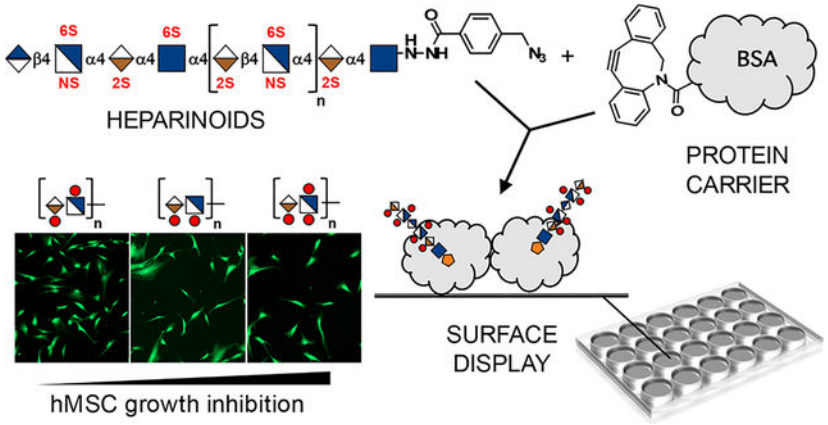

INTRODUCTION

The regulation of growth factor (GF) associated cellular proliferation and differentiation continues to be the focus of intense research in the areas of tissue engineering and regenerative medicine.[1] Integral to these efforts is the development of new biomaterials capable of delivery and tuning of GF activity in the cellular context.[2] The functions of GFs are influenced by the extracellular matrix (ECM) microenvironment, which is abundant in sulfated glycosaminoglycan (GAG) polysaccharides, such as heparan sulfate (HS), attached to core polypeptide backbones of proteoglycans (PGs). HS is a polymer composed of disaccharide repeat units of glucosamine and uronic acid modified by sulfate groups on specific nitrogen and oxygen atoms, which provide high-affinity binding sites for various GFs and modulate their activity (Figure 1).[3,4] While the arrangement of sulfation patterns in HS provides a molecular basis for affinity and selectivity in GF binding, the distribution of these molecules across the cell–matrix interface determines whether a GF signaling event will be promoted or attenuated (Figure 1). In the cellular glycocalyx, cell surface PG-associated HS promotes GF interactions with membrane receptors; however, when shed and deposited into the ECM, HS can sequester GFs away from the cell surface and downregulate signaling (Figure 1).[5] Consequently, HS offers a useful, tunable element for controlling GF-mediated signaling, provided that its influence on cellular activity is properly considered in the context of their presentation within the cellular microenvironment.[6,7]

While approaches for tailoring GAG-GF interactions directly within the cellular glycocalyx have begun to emerge,[8–10] more commonly GAGs are integrated into biomaterials for ECM engineering applications.[7] Heparin, a highly sulfated analogue of HS with affinity for a broad spectrum of GFs, has been a popular choice for a functional component in biomaterials for GF delivery and release.[7,11–13] The biological activities of heparin (**hep**) can be modulated through selective chemical desulfation[14] at the C6 hydroxyl of glucosamine (**6ODSH**), C2 hydroxyl of iduronic acid (**2ODSH**), or at the C2 nitrogen atom of glucosamine (**NDSH**, Figure 1). Reacetylation of the free amine groups in NDSH, which still contains 2-*O*- and 6-*O*-sulfates, then gives rise to the heparin analog, **NAcH** (Figure 1). The removal of sulfates from heparin alters the ability of the resulting heparinoids to engage GFs. For instance, the binding of the fibroblast growth factor 2 (FGF2) decreases in the

following order: **hep > 6ODSH > 2ODSH ≫ NDSH ~ NAcH**.[15] Therefore, these polysaccharides are well-suited as components for biomaterials to control FGF2 activity and the associated cell mitogenicity and proliferation.

Soluble heparin and HS GAGs can be physically entrapped within polymer networks,[16] adsorbed nonspecifically on polycationic surfaces (e.g., poly(L-lysine)),[17] or captured selectively on substrates coated with HS-binding peptides.[18,19] Covalent modifications of biomaterials with GAGs to generate more chemically stable systems with tunable properties and GF association can also be exploited to control cellular behavior.[20–24] The most commonly used strategy for covalent incorporation of GAGs into biomaterials makes use of the preponderance of carboxylic acid groups or, to a lesser extent, amino groups released by chemical *N*-desulfation along the polysaccharide chain, which are both suitable for conjugation via amide bond formation (Figure 2).[25–27] The high frequencyof these reactive side-chain groups limits control over the number and location of covalent modifications with individual polysaccharide molecules and may obscure sulfated regions required for HS bioactivity. Alternatively, amino acid residues that remain at the reducing ends of GAGs released from proteoglycans by peptidase treatment can be modified selectively under mild conditions using amide coupling conditions;[28] however, GAGs are often subjected to β-elimination to remove the peptide fragments and expose the glycan reducing end, thus limiting the generality of this approach. The unique reactivity of the reducing end offers an opportunity for single regiospecific chain functionalization outside of the sulfated regions via reductive amination (Figure 2)[29,30] or ligation with α-heteroatom nucleophiles, such as oximes or hydrazides.[25] Due to the requirement for large amounts of polysaccharides for their coupling to other macromolecules, these methods are often not amenable to the conjugation of scarcely available GAGs.

In order to remedy the issues of GAG presentation and glycan economy posed by the currently used conjugation techniques, we turned our sights toward the use of “click” chemistries. Bioorthogonal chemical ligation strategies, such as the copper-catalyzed[31] or strain-promoted[32] alkyne–azide cycloaddition (CuAAC and SPAAC, respectively) between alkynes and organic azides, exhibit fast kinetic profiles that allow for the efficient joining of biomacromolecules,[33,34] including GAGs,[35–38] under physiological conditions. A mild chemoselective strategy for covalently linking GAGs to proteins would expand the utility of these biologically important molecules in ECM engineering, as large comprehensive libraries of structurally well-defined GAG oligo- and polysaccharides are becoming increasingly available through chemoenzymatic synthesis[39] and glycosylation engineering.[40–42] Here, we report an efficient method for the ligation of variously sulfated heparinoids to protein carriers using a SPAAC-based conjugation strategy (Figure 2). We demonstrate the utility of the resulting bioconjugates as ECM proteoglycan models capable of controlling FGF2 activity and human mesenchymal stem cell (hMSC) proliferation in culture according to their patterns of sulfation.

RESULTS AND DISCUSSION

We initiated our study by identifying conditions under which a hydrazide ligation to the reducing ends of HS chains could serve as an efficient chemo- and regioselective method for

the formation of heparinoid–protein conjugates. The direct coupling of heparinoids to macromolecules chemically modified to present hydrazide groups generally suffers from low efficiency.[25] Under equilibrium, the formation of the hydrazone adduct is disfavored by the low concentration of the reactive aldehyde form of the polysaccharide reducing end as well as by the size of the two macromolecular coupling partners, which is exacerbated by the high negative charge density of the HS polysaccharides. We reasoned that the conjugation process would be more effective if it were accomplished in two steps by first priming the GAG chain reducing end with a small azide-containing handle followed by coupling to cyclooctyne-modified proteins via the rapid and irreversible SPAAC reaction.

Using heparin (Mw ~ 12 kDa) as a model for HS GAGs, we first optimized the chain-end prefunctionalization step (Figure 3A). Priming of heparin was achieved by heating the polysaccharide with 4-azidomethyl benzhydrazide[43] (**1**, 6.5 equiv) at 50 °C for 72 h under acidic conditions (1:1 acetate buffer/DMSO, pH = 5.5). After neutralization, the heparin derivative was purified by dialysis against water to remove unreacted linker **1**, salts, and the DMSO cosolvent. ^{1}H NMR analysis of the purified heparin product **2-hep** in D_2O clearly indicated the presence of a new broad signal at $\delta \sim 7.5$ ppm corresponding to the aromatic protons of the 4-azidomethyl benzhydrazide end group (Figure S4); however, the low abundance of the end modification NMR signals with respect to those of the heparin polysaccharide chain made accurate determination of the reaction efficiency difficult. The reaction conditions were also effective for introducing the azidomethyl benzyhrazide handle into commercially available **6ODSH**, **2ODSH**, **NDSH**, and **NAcH** heparin derivatives derived by chemical desulfation of the parent heparin polysaccharide (Figures S5–8).

Having derived chemically primed heparinoids **2**, we next evaluated the SPAAC conjugation of the azide-terminated heparin (**2-hep**) to bovine serum albumin (BSA), a model protein carrier, modified with complementary cyclooctyne functionality (Figure 3A). We chose BSA based on its previously demonstrated suitability for the generation of synthetic neoglyconjugates.[44–46] The treatment of BSA with dibenzocyclooctyne-PEG_4-*N*-hydroxysuccinimidyl ester (DBCO-PEG_4-NHS, 8 equiv) in sodium bicarbonate buffer (100 mM, pH = 8.0) overnight resulted in covalent functionalization of solvent exposed lysine side chains in BSA. MALDI analysis of the resulting DBCO-BSA conjugate **3** indicated the introduction of ~6 DBCO residues per BSA molecule (Figure 3B). The DBCO-BSA conjugate **3** can be further treated with NHS-biotin (21 equiv) in bicarbonate buffer (100 mM, pH = 8.0) overnight to incorporate biotin handles for quantification in downstream applications (**3-biotin**, ~19 biotins per BSA by MALDI, Figure S10).

The appropriately functionalized azide-heparin (**2-hep**) and DBCO-BSA (**3**) coupling partners could now be joined together to generate the desired heparin–BSA conjugate. The two components (0.5 μM, 1 equiv of **2-hep** per DBCO residues in **3**) were allowed to react in PBS at ambient temperature for 48 h. The crude heparin–BSA (**hep-BSA**) adduct was purified by spin-dialysis (25 kDa MWCO) and ionexchange to remove unreacted **2-hep** and **3**, respectively, and analyzed by size exclusion chromatography (SEC, Figures 3C and S11). Composition analysis of the purified neoglycoprotein product using carbazole and BCA assays revealed that the reaction proceeded to completion. This garnered BSA molecules decorated with ~6 pendant heparin chains, matching the number of reactive cyclooctyne

residues in **3** (Figure S13). The remaining desulfated heparinoids **2** were subjected to the optimized coupling conditions to yield a panel of heparinoid-BSA conjugates (**6ODSH-**, **2ODSH-**, **NDSH-**, and **NAcH-BSA**). For biological experiments (*vide infra*), only partial purification of the crude bioconjugates by spin-filtration (25 kDa MWCO) was required to eliminate the contributions of unreacted heparinoids **2**, thus eliminating the need for laborious isolation sequences and large quantities of expensive or scarce GAG materials.

We envisioned that the new heparinoid–BSA conjugates could serve as ECM components for controlling the proliferation of hMSCs in culture by sequestering the proliferative signal, FGF2, away from its cell surface receptors. To test the ability of the conjugates to capture FGF2, we first immobilized **hep-BSA** at increasing concentration (1, 10, and 100 μg/mL based on BSA) on tissue culture-treated polystyrene 96 well plates. Using an ELISA format, the resulting heparin–BSA displays were probed with FGF2 (10 nM) and detected using a primary anti-FGF2 antibody followed by a secondary antibody–HRP conjugate in the presence of chromogenic reagent, TMB (Figure 4A). The immobilized **hep-BSA** captured FGF2 at all surface densities, reaching signal saturation in wells treated with 100 μg/mL of the conjugate (Figure 4B). Importantly, cross-examination of the SPAAC derived **hep-BSA** against heparin conjugates prepared using standard NHS-promoted amide coupling[47] (**hep-BSA-ac**) and reductive amination[48] (**hep-BSA-ra**) procedures revealed similar FGF2-binding ability for all three compounds (Figure S14).

To assess FGF2 capture in response to altered sulfation patterns, the differentially sulfated heparinoid–BSA conjugates were immobilized (100 μg/mL) and analyzed using ELISA (Figure 4C). In line with previous observations,[15] the 6-*O*- and 2-*O*-desulfated heparinoid conjugates (**6ODSH**-and **2ODSH-BSA**) showed decreased FGF2 binding compared to **hep-BSA**, while the *N*-desulfated analogs (**NDSH**- and **NAcH-BSA**) exhibited minimal avidity for the growth factor. It should be noted that the **2ODSH-BSA** conjugate retained surprisingly high FGF2 binding capacity, which may, presumably, be attributed to the relatively high overall sulfation level of the parent heparin compared to HS, in which the loss of 2-*O*-sufation ablates FGF2 binding.[15] The anti-HS antibody, 10E4, which recognizes predominantly *N*-sulfated HS GAGs, also detected the immobilized heparinoid conjugates according to their composition (Figure 4D), further confirming the sulfation pattern-dependent bioactivity of the materials. To ensure that the differential FGF2 and 10E4 binding reflected the unique heparinoid composition rather than unequal neoglycoconjugate immobilization, we employed a two-point assay using biotinylated heparinoid–BSA conjugates in conjunction with heparinase digest and glycan stub detection. ELISA analysis of the arrayed glycoconjugates with streptavidin-HRP revealed equal surface density of BSA (Figure S15). The conjugates were then treated with heparinase to depolymerize the GAG component. ELISA quantification using an anti-HS stub antibody, 3G10, indicated equal distribution of the remaining heparinoid fragments bound to the immobilized BSA (Figure S16). Collectively, these assays confirm uniform surface adsorption for all heparinoid–BSA conjugates, regardless of their level of sulfation and overall charge density.

HS GAGs deposited into the ECM by cells provide binding sites for a variety of GFs. There, they can serve a dual role as a depot for concentrating GF activity or as a local sink sequestering these biochemical cues away from cell surface receptors.[3] To assess the ability

of the newly generated heparinoid–BSA conjugates to function as ECM proteoglycan models, we tested their effects on FGF2-mediated hMSC proliferation *in vitro* (Figure 5). In this assay, hMSCs were seeded in 24 well tissue culture plates coated with heparinoid–BSA conjugates (100 μg/mL). The cells were allowed to proliferate for 3 days and proliferation rates were assessed by microscopy assisted cell counting (Days 0–3, Figure 5A, B and Figures S18 and S19) and by the incorporation of radioactive [^{3}H]thymidine into newly synthesized DNA (Day 3, Figure 5C and Figures S17 and S20). While the glycoconjugate composition had no effect on hMSC seeding and adhesion compared to control BSA-coated wells (Day 0, Figure S18), we observed significant attenuation of cell proliferation concurring with the ability of the immobilized heparinoid conjugates to capture FGF2 (Figures 5 and 4). Accordingly, **hep-BSA** coating exhibited maximal proliferation inhibition (~2-fold, Figures 5 and S20), followed by **6ODSH**- and **2ODSH-BSA** conjugates, while **NDSH**- and **NAcH-BSA** conjugates showed no appreciable effect on cell proliferation compared to BSA-treated surfaces. Supplementation of the culture medium with soluble heparin (100 μg/mL) or the FGFR kinase inhibitor, PD173074 (10 nM), inhibited hMSC proliferation to a similar extend as immobilized **hep-BSA** (Figure S20). Heparinase treatment of the immobilized **hep-BSA** conjugate to remove the GAG component fully restored hMSC proliferation (Figure S21). These control conditions provided support for the conclusion that proliferation inhibition on heparinoid surfaces resulted from the attenuation of FGF2 activity.

These findings need to be brought into context with prior observations reporting on enhanced proliferation of hMSC produced with heparin-coated chitosan surfaces,[27] heparin-functionalized PEG hydrogels,[22] or with surfaces modified with HS-binding peptides.[13] In these studies, the positive effects on cell proliferation were postulated to arise from improved cell adhesion and spreading on the substrates in the presence of heparin or HS and the ability of the glycans to concentrate exogenous FGF2 from the growth media. In contrast, the present study evaluated the ability of the heparinoid conjugates to influence hMSC proliferation by acting as localized sink for FGF2 present in the cell culture medium (~30–50 ng/L) while exhibiting similar cell adhesion properties (Figure 5B and Figure S18). Given the dual role of ECM HS to act as both a sink and a depot for GFs, we anticipate that the bioactivity of the heparinoid–BSA conjugates will be context-dependent and determined by the concentration of GFs in media relative to the binding capacity of the immobilized glycoconjugates.

In conclusion, we have developed an efficient method for generating and presenting heparinoid–protein conjugates. The neoglycoproteins were prepared using a two-step process, in which the reducing ends of HS GAG polysaccharides were prefunctionalized with reactive azide handles via a chemoselective hydrazide ligation for a subsequent coupling to cyclooctyne modified BSA. When adsorbed on the surface of polystyrene tissue culture plates, the conjugates provided extracellular environments with capacity to bind and sequester FGF2 according to the sulfation patterns of their pendant glycans and downregulate stem cell proliferation. The mild bioconjugation conditions and glycan economy make this method well suited for expanding the diversity of the

neoglycoconjugates with respect to both the protein and glycan components, including GAGs derived in small quantities from biological samples.

METHODS

Materials.

All chemicals, unless stated otherwise, were purchased from Sigma-Aldrich and used as received. A complete list of biological reagents and materials is provided in Table S1 in the Supporting Information. Heparin and desulfated heparinoids were purchased from Iduron (Manchester, UK). The chemically desulfated heparinoids used in this study originated from the unmodified heparin. The disaccharide analysis of the heparin and desulfated heparins was provided Iduron and is in Figure S1. The major (>75%) unit of heparin is the trisulfated disaccharide, IdoA(2S)-GlcNS(6S). Chemical desulfation resulted in 6ODSH (~90% reduction in 6-*O*-sulfates and ~25% loss of 2-*O*-sulfates), 2ODSH (~95% reduction in 2-*O*-sulfates), NDSH, and NAcH (~90% reduction in *N*-sulfate).

Instrumentation.

Nuclear magnetic resonance (NMR) spectra were collected on a Bruker 300 MHz NMR spectrometer. Spectra are reported in parts per million (ppm) on the δ scale relative to the residual solvent as an internal standard. Size exclusion chromatography (SEC) was performed on a Hitachi Chromaster system equipped with an RI detector and an 8 μm, mixed bed, 300 × 7.5 mm cm PL aquagel–OH mixed medium column. 96-well plate assays (ELISA, carbazole) were analyzed using a Varioskan LUX multimode microplate reader. Matrix-assisted laser desorption ionization coupled with time-of-flight (MALDI-TOF) analysis was acquired via a Bruker Biflex IV MALDI-TOF MS in positive ion mode using sinapinic acid matrix. Bright field and fluorescence microscopy images were taken using ZEISS Axio Observer microscope. Radioactive thymidine assays were analyzed using a Beckman Coulter LS6500 Liquid Scintillation Counter.

Synthesis of End-Functionalized Heparinoids 2.

In a PCR tube, heparin (6.0 mg, 0.5 μmol) was dissolved in sodium acetate buffer (100 mM, 53.4 μL, pH 5.5) containing aniline (100 mM). In a separate PCR tube, 4-(azidomethyl)-benzhydrazide (6.0 mg, 31.4 μmol, 6.4 equiv) was dissolved in DMSO (30.0 μL) and added to the heparin solution. The PCR tube containing the final mixture was then capped, placed into a thermocycler set to 50 °C and heated for 72 h. After this time, the reaction mixture was diluted with PBS (~7.0 mL) and dialyzed in SnakeSkin dialysis tubing (3.5 kDa MWCO) against MQ water for 48 h, replacing the MQ water after 24 h. The dialyzed product was lyophilized to afford the end-chain modified heparin product, **2-hep** (6.0 mg, quatitative recovery). Heparinoids **2** were prepared and purified using an identical procedure.

Synthesis of DBCO-BSA Conjugate 3.

In a 1.5 mL microcentrifuge tube, BSA (10.0 mg) was dissolved in sodium bicarbonate buffer (100 mM, 1.0 mL, pH = 8.3). A solution of dibenzocyclooctyne-PEG4-*N*-hydroxysuccinimidyl ester in DMSO (10.0 mg/mL, 78.0 μL, 8.0 equiv) was added and the

reaction was stirred at 4 °C overnight. After this time, the reaction mixture was transferred into dialysis tubing (25 kDa MWCO) and dialyzed against MQ water for 48 h, replacing water after 24 h. The dialyzed DBCO-BSA product **3** was lyophilized to afford white solid (11.0 mg, 94% mass recovery). The product **3** was analyzed by MALDI-TOF (m/z = 70,803) indicating the addition of an average of ~6 DBCO modifications per molecule of BSA.

Heparin-/Heparinoid-BSA Conjugation via SPAAC.

To a 1.5 mL microcentrifuge tube charged with azide end-prefunctionalized heparin **2-hep** (6.0 mg, 0.5 μmol) was added a solution of DBCO-BSA conjugate **3** in PBS (10.0 mg/mL, 600.0 μL, 1 equiv per DBCO). The reaction was allowed to proceed at RT for 48 h. After this time, the conjugate was diluted to a total volume of 4 mL with aqueous solution of NaCl (1.5 M) and spin-dialized (30 kDa MWCO, 4000*g*, 20 min). This was repeated a second time with the NaCl solution and 4 more times with MQ water. After this treatment, all unconjugated heparin was removed leaving behind **hep-BSA** with some amount of unreacted DBCO-BSA conjugate **3**, as evidenced by SEC analysis (Figure S11). The product was lyophilized to afford a white solid **hep-BSA** conjugate (11.0 mg, quantitative mass recovery by BSA), which was used directly for biological experiments or purified further for compositional analysis by size exclusion and ion exchange chromatography to remove **3**. Heparinoid–BSA conjugates were synthesized using an identical procedure.

Surface Immobilization of Heparinoid–BSA Conjugates.

A 1.0 mg/mL heparinoid–BSA conjugate solution in PBS was filtered through a 0.22 μm sterile filter and 50.0 μL of the solution was added per well of a 24 well plate. The solution was spread using the back of a p200 pipet tip to fully cover the well surface. The plate was dried and further sterilized overnight under UV irradiation. The plate was then washed 3 times with PBS before being used for cellular experiments. When immobilizing conjugates in a 96 well plate for ELISA, wells were treated with 13 μL/well of a heparinoid–BSA conjugate in PBS. The plate was centrifuged at 70g for 3 min to spread the solution evenly within the well. The coated 96 well plate was left at RT to dry overnight. The plate was washed six times using 200 μL PBS with 2 min of rocking per wash prior to use. Both 24 and 96 well plates were composed of the same tissue culture treated plastic.

FGF2 Binding Assay.

The wells of a 96 well plate were coated with heparinoid–BSA conjugates as described above. After blocking with 2% BSA solution in PBS for 1 h at RT, the blocking solution was removed and the wells were incubated with a solution of FGF2 (10 nM) in 1% BSA/PBS for 1 h at RT. After incubation, the wells were washed 6 times with 200 μL PBS containing 0.1% v/v Tween 20 with rocking for 2 min per wash. The wells were washed again 6 times with 200 μL PBS with rocking for 2 min per wash. To the washed wells was added a solution of primary anti-FGF2 antibody in 1% BSA/PBS (1:1000 dilution). After 1 h incubation at RT, the wells were washed 6 times with 200 μL of PBS containing 0.1% v/v Tween 20 with rocking for 2 min per wash. The wells were treated with a solution of secondary antibody–HRP conjugate in 1% BSA/PBS (1:3000 dilution) at RT for 1 h. After incubation, the wells were washed 6 times with 200 μL of PBS containing 0.1% v/v Tween

20 with rocking for 2 min per wash. Then, a TMB solution (100 μL) was added, and after 5 min, the peroxidase reaction was developed with 2 N sulfuric acid and the absorbance at 450 nm was measured on a plate reader.

General Cell Culture Procedures.

Bone marrow derived human mesenchymal stem cells (hMSCs) were maintained in MSC medium containing rh-FGF2 (5 ng/mL), rh-IGF1 (15 ng/mL), L-alanyl-L-glutamine, 7% FBS, and penicillin/streptomycin (1:100). The cells were grown in monolayer culture in tissue culture treated T25 flasks at 37 °C, 5% CO_2. Media was changed every 3 days of growth and the cells were passaged every 6 days at a ratio of 1:10 after dissociation with 0.05% trypsin-EDTA at 37 °C, 5% CO_2, which was neutralized with an equal volume of growth medium. Cells were washed with PBS after the removal of old media. Cells were used for experiments when they reached passage 6. All cellular experiments took place in 24 well tissue culture plates. Statistical analysis was performed using Prism software. Error bars refer to standard deviation from the mean and p values were calculated using a one-way ANOVA, $p^* < 0.05$, $p^{***} < 0.001$.

Cell proliferation Assay.

In a 24 well plate, hMSCs were seeded in MSC growth medium in wells coated with heparinoid–BSA conjugates at a seeding density of 2,500 cells/cm^2. The cells were allowed to adhere for 18 h, after which the cells were washed once with PBS and then cultured in α-MEM medium supplemented with 10% FBS and penicillin/streptomycin (1:100) on Day 0. Control condition cells were seeded in wells coated with BSA alone and treated in the presence or absence of soluble heparin (100 μg/mL) or PD173074 (10 nM). On Day 2, [^{3}H]thymidine (0.5 μCi) was added to each well in a total volume of 10 μL in PBS and the cells were cultured for additional 24 h. On Day 3, the media were removed, cells were washed 3 times with PBS and lysed in a lysis buffer (400 μL, 0.1 M NaOH, 0.1% w/v sodium dodecyl sulfate). The radioactive lysate (300 μL) was transferred to a scintillation vial containing 5 mL of Ultima Gold liquid scintillation fluid and analyzed using a liquid Scintillation counter. For assessment of proliferation via cell counting, 3 random viewing frames per well were acquired using phase microscopy at 100× magnification and the cells were counted. Counting was repeated daily, and on Day 3, the cells were live-stained with Calcein AM (1 μM in PBS) to enhance the accuracy of counting, as the cells become more confluent and less easily distinguished from one another.

Supplementary Material

Refer to Web version on PubMed Central for supplementary material.

ACKNOWLEDGMENTS

We thank the Glycobiology Research and Training Center for access to tissue culture facilities and analytical instrumentation. This work was supported by the NIH Director's New Innovator Award (NICHD: 1DP2HD087954-01). P.L.S.M. was supported by the UCSD/UCLA Diabetes Research Center grant P30 DK063491. K. G. is supported by the Alfred P. Sloan Foundation (FG-2017-9094) and the Research Corporation for Science Advancement via the Cottrell Scholar Award (grant # 24119)

REFERENCES

(1). Lutolf MP, and Hubbell JA (2005) Synthetic biomaterials as instructive extracellular microenvironments for morphogenesis in tissue engineering. Nat. Biotechnol 23, 47–55. [PubMed: 15637621]

(2). Lee K, Silva EA, and Mooney DJ (2011) Growth factor delivery-based tissue engineering: general approaches and a review of recent developments. J. R. Soc., Interface 8, 153–170. [PubMed: 20719768]

(3). Xu D, and Esko JD (2014) Demystifying heparin sulfate-protein interactions. Annu. Rev. Biochem 83, 129–157. [PubMed: 24606135]

(4). Pomin VH (2016) Paradigms in the structural biology of the mitogenic ternary complex FGF:FGFR:heparin. Biochimie 127, 214–26. [PubMed: 27263122]

(5). Vlodavsky I, Bar-Shavit R, Ishar-Michael R, Bashkin P, and Fuks Z (1991) Extracellular sequestration and release of fibroblast growth factor: a regulatory mechanism? Trends Biochem. Sci 16, 268–271. [PubMed: 1926336]

(6). Ayerst BI, Merry CLR, and Day AJ (2017) The good the bad and the ugly of glycosaminoglycans in tissue engineering applications. Pharmaceuticals 10, 54.

(7). Hudalla GA, and Murphy WL (2011) Biomaterials that regulate growth factor activity via bioinspired interactions. Adv. Funct. Mater 21, 1754–1768. [PubMed: 21921999]

(8). Huang ML, Smith RAA, Trieger GW, and Godula K (2014) Glycocalyx remodeling with proteoglycan mimetics promotes neural specification in embryonic stem cells. J. Am. Chem. Soc 136, 10565–8. [PubMed: 25019314]

(9). Naticchia MR, Laubach LL, Tota EM, Lucas TM, Huang ML, and Godula K (2018) Embryonic stem cell engineering with a glycomimetic FGF2/BMP4 co-receptor drives mesodermal differentiation in a three-dimensional culture. ACS Chem. Biol 13, 2880. [PubMed: 30157624]

(10). Pulsipher A, Griffin MA, Stone SE, and Hsieh-Wilson LC (2015) Long-lived glycan engineering to direct stem cell fate. Angew. Chem., Int. Ed 54, 1466–1470.

(11). Liang Y, and Kiick KL (2014) Heparin-functionalized polymeric biomaterials in tissue engineering and drug delivery applications. Acta Biomater. 10, 1588–1600. [PubMed: 23911941]

(12). Martino MM, Briquez PS, Ranga A, and Hubbell JA (2013) Heparin-binding domain of fibrin(ogen) binds growthfactors and promotes tissue repair when incorporated within a synthetic matrix. Proc. Natl. Acad. Sci. U. S. A 110, 4563–4568. [PubMed: 23487783]

(13). Hudalla GA, Kouris NA, Koepsel JT, Ogle BM, and Murphy WL (2011) Harnessing endogenous growth factor activity modulates stem cell behavior. Integr. Biol 3, 832–42.

(14). Roy S, Lai H, Zouaoui R, Duffner J, Zhou H, P Jayaraman L, Zhao G, Ganguly T, Kishimoto TK, and Venkataraman G (2011) Bioactivity screening of partially desulfated low-molecular-weight heparins: a structure/activity relationship study. Glycobiology 21, 1194–205. [PubMed: 21515908]

(15). Lundin L, Larsson H, Kreuger J, Kanda S, Lindahl U, Salmivirta M, and Claesson-Welsh L (2000) Selectively desulfated heparin inhibits fibroblast growth factor-induced mitogenicity and angiogenesis. J. Biol. Chem 275, 24653–24660. [PubMed: 10816596]

(16). Sterner E, Meli L, Kwon SJ, Dordick SJ, and Linhardt JR (2013) FGF-FGFR signaling mediated through glycosaminogly-cans in microtiter plate and cell-based microarray platforms. Biochemistry 52, 9009–9019. [PubMed: 24289246]

(17). Rogers CJ, Clark PM, Tully SE, Abrol R, Garcia KC, Goddard WA III, and Hsieh-Wilson LC (2011) Elucidating glycosaminoglycan–protein–protein interactions using carbohydrate microarray and computational approaches. Proc. Natl. Acad. Sci. U. S.A. 108, 9747–9752. [PubMed: 21628576]

(18). Klim RJ, Li L, Wrighton JP, Piekarczyk SM, and Kiessling LL (2010) A defined glycosaminoglycan-binding substratum for human pluripotent stem cells. Nat. Methods 7, 989. [PubMed: 21076418]

(19). Hudalla GA, Koepsel JT, and Murphy WL (2011) Surfaces that sequester serum-borne heparin amplify growth factor activity. Adv. Mater 23, 5415–5418. [PubMed: 22028244]

(20). Freudenberg U, Zieris A, Chwalek K, Tsurkan MV, Maitz MF, Atallah P, Levental KR, Eming SA, and Werner C (2015) Heparin desulfation modulates VEGF release and angiogenesis in diabetic wounds. J. Controlled Release 220, 79–88.

(21). Xu X, Jha AK, Duncan RL, and Jia X (2011) Heparin-decorated, hyaluronic acid-based hydrogel particles for the controlled release of bone morphogenetic protein 2. Acta Biomater. 7, 3050–3059. [PubMed: 21550426]

(22). Benoit DS, and Anseth KS (2005) Heparin functionalized PEG gels that modulate protein adsorption for hMSC adhesion and differentiation. Acta Biomater. 1, 461–470. [PubMed: 16701827]

(23). Mathews S, Mathew SA, Gupta PK, Bhonde R, and Totey SJ (2014) Glycosaminoglycans enhance osteoblast differentiation of bone marrow derived human mesenchymal stem cells. J. Tissue Eng. Regener. Med 8, 143–152.

(24). Zieris A, Dockhorn R, Röhrich A, Zimmermann R, Müller M, Welzel PB, Tsurkan MV, Sommer JU, Freudenberg U, and Werner C (2014) Biohybrid networks of selectively desulfated glycosaminoglycans for tunable growth factor delivery. Biomacromolecules 15, 4439–4446. [PubMed: 25329425]

(25). Köwitsch A, Zhou G, and Groth T (2018) Medical application of glycosaminoglycans: a review. J. Tissue Eng. Regener. Med 12, e23–41.

(26). Zieris A, Dockhorn R, Röhrich A, Zimmermann R, Müller M, Welzel PB, Tsurkan MV, Sommer JU, Freudenberg U, and Werner C (2014) Biohybrid networks of selectively desulfated glycosaminoglycans for tunable growth factor delivery. Biomacromolecules 15, 4439–4446. [PubMed: 25329425]

(27). Uygun BE, Stojsih SE, and Matthew HW (2009) Effects of immobilized glycosaminoglycans on the proliferation and differentiation of mesenchymal stem cells. Tissue Eng., Part A 15, 3499–3512. [PubMed: 19456238]

(28). Pulsipher A, Griffin ME, Stone SE, Brown JM, and Hsieh-Wilson LC (2014) Directing neuronal signaling through cell-surface glycan engineering. J. Am. Chem. Soc 136, 6794–6797. [PubMed: 24746277]

(29). Zhang F, Fath M, Marks R, and Linhardt R (2002) A highly stable covalent conjugated heparin biochip for heparin–protein interaction studies. Anal. Biochem 304, 271–273. [PubMed: 12009707]

(30). Gildersleeve JC, Oyelaran O, Simpson JT, and Allred B (2008) Improved procedure for direct coupling of carbohydrates to proteins via reductive amination. Bioconjugate Chem. 19, 1485–1490.

(31). Kolb HC, Finn MG, and Sharpless KB (2001) Click chemistry: diverse chemical function from a few good reactions. Angew. Chem., Int. Ed 40, 2004–2021.

(32). Jewett JC, and Bertozzi CR (2010) Cu-free click cycloaddition reactions in chemical biology. Chem. Soc. Rev 39, 1272–1279. [PubMed: 20349533]

(33). Spicer CD, Pashuck ET, and Stevens MM (2018) Achieving controlled biomolecule-biomaterial conjugation. Chem. Rev 118, 7702–7743. [PubMed: 30040387]

(34). He XP, Zeng YL, Zang Y, Li J, Field RA, and Chen GR (2016) Carbohydrate CuAAC click chemistry for therapy and diagnosis. Carbohydr. Res 429, 1–22. [PubMed: 27085906]

(35). Fajardo AR, Guerry A, Britta EA, Nakamura CV, Muniz EC, Borsali R, and Halila S (2014) Sulfated glycosaminoglycan-based block copolymer: preparation of biocompatible chondroitin sulfate b poly(lactic acid) micelles. Biomacromolecules 15, 2691–2700. [PubMed: 24857763]

(36). Upadhyay KK, Le Meins J-F, Misra A, Voisin P, Bouchaud V, Ibarboure E, Schatz C, and Lecommandoux S (2009) Biomimetic doxorubicin loaded polymersomes from hyalur-onan-block-poly(γ-benzyl glutamate) copolymers. Biomacromolecules 10, 2802–2808. [PubMed: 19655718]

(37). Yamaguchi M, Kojima K, Hayashi N, Kakizaki I, Kon A, and Takagaki K (2006) Efficient and widely applicable method of constructing neo-proteoglycan utilizing copper(I) catalyzed 1,3-dipolar cycloaddition. Tetrahedron Lett. 47, 7455–7458.

(38). van Kuppevelt TH, Oosterhof A, Versteeg EMM, Podhumljak E, van de Westerlo EMA, and Daamen WF (2017) Sequencing of glycosaminoglycans with potential to interrogate sequence-specific interactions. Sci. Rep 7, 14785. [PubMed: 29093576]

(39). DeAngelis PL, Liu J, and Linhardt RJ (2013) Chemoenzymatic synthesis of glycosaminoglycans: re-creating, remodeling and re-designing nature's longest or most complex carbohydrate chains. Glycobiology 23, 764–777. [PubMed: 23481097]

(40). Chen Y, Narimatsu Y, Clausen TM, Gomes C, Karlsson R, Steentoft C, Spliid CB, Gustavsson T, Salanti A, and Persson A (2018) The GAGOme: a cell-based library of displayed glycosaminoglycans. Nat. Methods 15, 881. [PubMed: 30104636]

(41). Qiu H, Shi S, Yue J, Xin M, Nairn AV, Lin L, Liu X, Li G, Archer-Hartmann SA, Dela Rosa M, Galizzi M, Wang S, Zhang F, Azadi P, van Kuppevelt TH, Cardoso WV, Kimata K, Ai X, Moremen KW, Esko JD, Linhardt RJ, and Wang L (2018) A mutant-cell library for systematic analysis of heparan sulfate structure-function relationships. Nat. Methods 15, 889–899. [PubMed: 30377379]

(42). Baik JY, Gasimli L, Yang B, Datta P, Zhang F, Glass CA, Esko JD, Linhardt RJ, and Sharfstein ST (2012) Metabolic engineering of Chinese hamster ovary cells: towards a bioengineered heparin. Metab. Eng 14, 81–90. [PubMed: 22326251]

(43). Smith JM, Vitali F, Archer SA, and Fasan R (2011) Modular assembly of macrocyclic organo–peptide hybrids using synthetic and genetically encoded precursors. Angew. Chem., Int. Ed 50, 5075–5080.

(44). Laaf D, Bojarová P, Pelantová H, Křen V, and Elling L (2017) Tailored multivalent neo-glycoproteins: synthesis, evaluation, and application of a library of galectin-3-binding glycan ligands. Bioconjugate Chem. 28, 2832–2840.

(45). Prasanphanich NS, Song X, Heimburg-Molinaro J, Luyai AE, Lasanajak Y, Cutler CE, Smith DF, and Cummings RD (2015) Intact reducing glycan promotes the specific immune response to lacto-N-neotetraose-BSA neoglycoconjugates. Bioconjugate Chem. 26, 559–571.

(46). Zhang Y, Li Q, Rodriguez LG, and Gildersleeve JC (2010) An array-based method to identify multivalent inhibitors. J. Am. Chem. Soc 132, 9653–9662. [PubMed: 20583754]

(47). Hermanson GT (2013) Zero length crosslinkers, in Bioconjugate Techniques, 3rd ed., Chapter 4.1, Academic Press.

(48). Uchimura K, Morimoto-Tomita M, Bistrup A, Li J, Lyon M, Gallagher J, Werb Z, and Rosen SD (2006) HSulf-2, an extracellular endoglucosamine-6-sulfatase, selectively mobilizes hep-arin-bound growth factors and chemokines: effects on VEGF, FGF-1, and SDF-1. BMC Biochem. 7, 2. [PubMed: 16417632]

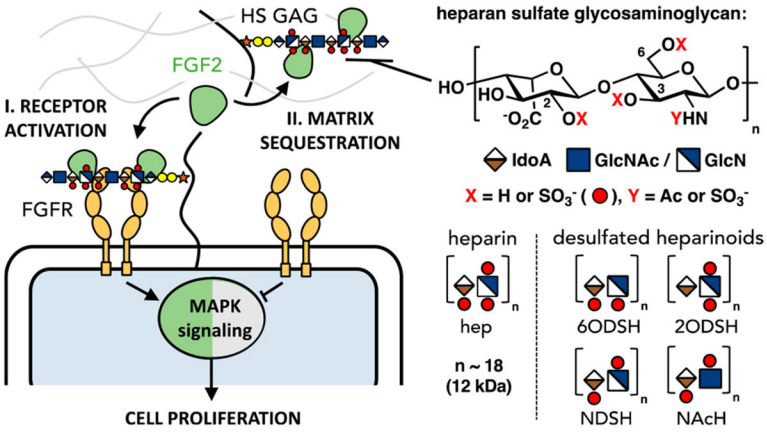

Figure 1.

Heparan sulfate (HS) glycosaminoglycans (GAGs) regulate FGF2 activity at the cellular boundary. Cell surface HS facilitates the activation of FGF receptors (FGFRs) and promotes cell proliferation. Extracellular matrix (ECM) HS sequesters FGF2 away from the cell surface and inhibits proliferation. Selective chemical desulfation of heparin, a highly sulfated HS, yields heparinoids with distinct FGF2 binding profiles.

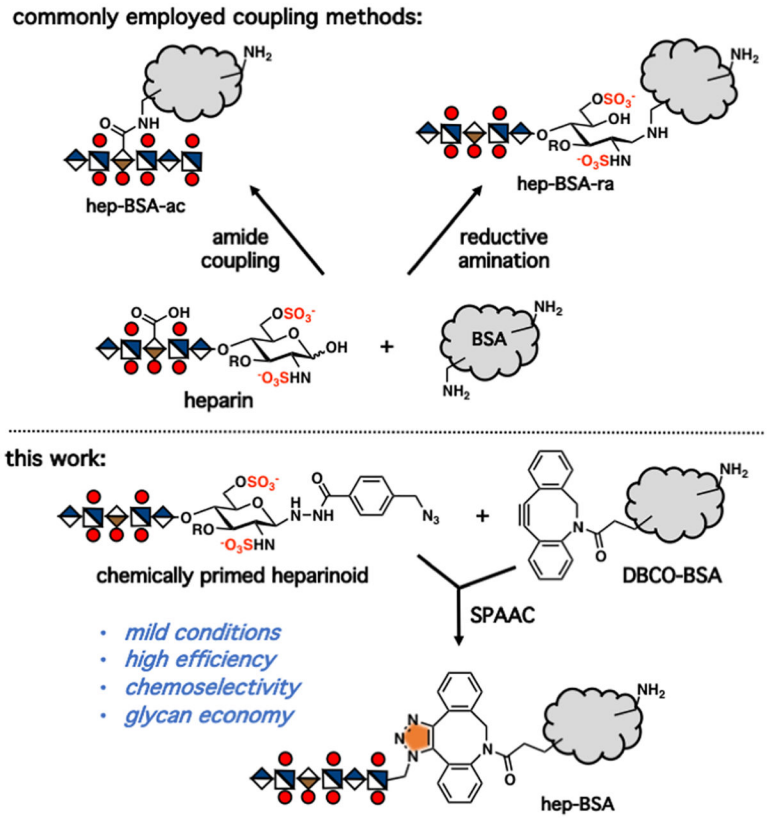

Figure 2.

Common techniques for generating heparin bioconjugates include cross-linking of solvent exposed lysine residues on proteins (e.g., BSA) with either pendant carboxylic acid groups along the polysaccharide chain (amide coupling) or through its reducing end (reductive amination). The strain-promoted alkyne–azide cycloaddition (SPAAC) between chemically primed heparinoids and cyclooctyne-modified proteins offers a highly efficient chemoselective alternative to the existing methods.

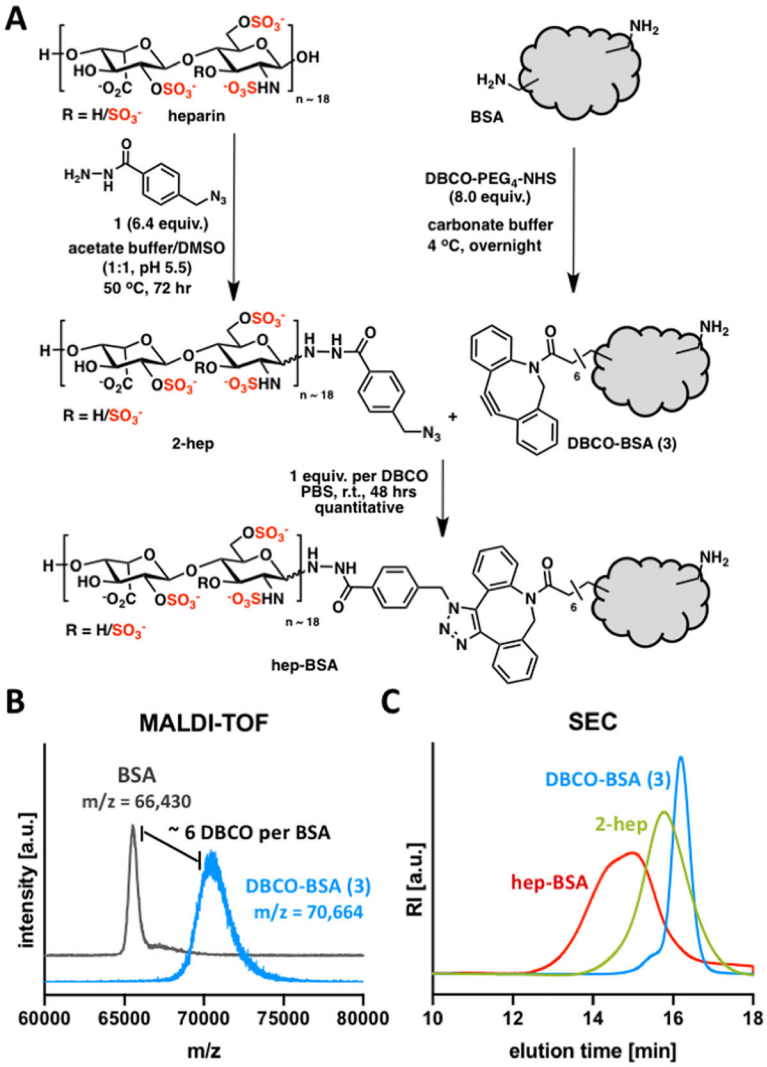

Figure 3.

Synthesis and characterization of heparin–BSA conjugate (**hep-BSA**). (A) **Hep-BSA** synthesis via a reducing end priming with azidomethyl benzhydrazide (**1**) followed by SPAAC reaction between the resulting azido-heparin (**2-hep**) and DBCO-BSA (**3**). (B) MALDI analysis of **3** indicated ~6 DBCO groups per BSA molecule. (C) SEC traces for 3 (blue), **2-hep** (green), and purified **hep-BSA** (red).

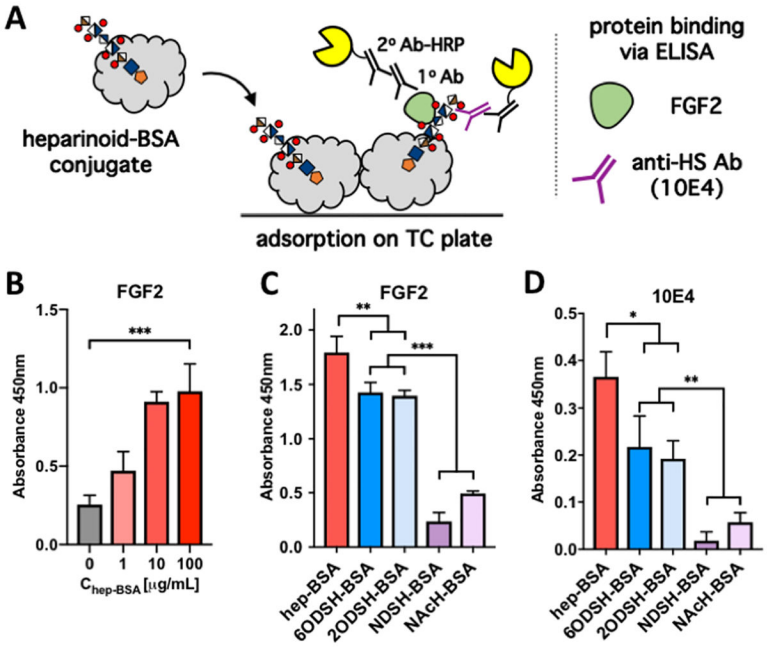

Figure 4.

Immobilized heparinoid–BSA conjugates are recognized by proteins based on their sulfate composition. (A) The conjugates were adsorbed on polystyrene tissue culture (TC) plates and evaluated for the binding of FGF2 (10 nM) and the anti-HS antibody, 10E4 (1:1000 dilution), using ELISA. (B) Maximum FGF2 binding was observed for hep-BSA immobilized at 100 μg/mL concentration. (C,D) Removal of 6-*O*-, 2-*O*-, and *N*-sulfation in immobilized heparinoid–BSA conjugates (100 μg/mL) led to increasing loss of FGF2 and 10E4 binding. (ANOVA, Tukey's multiple comparisons test; $p^* < 0.05$, $p^{**} < 0.01$, $p^{***} < 0.001$).

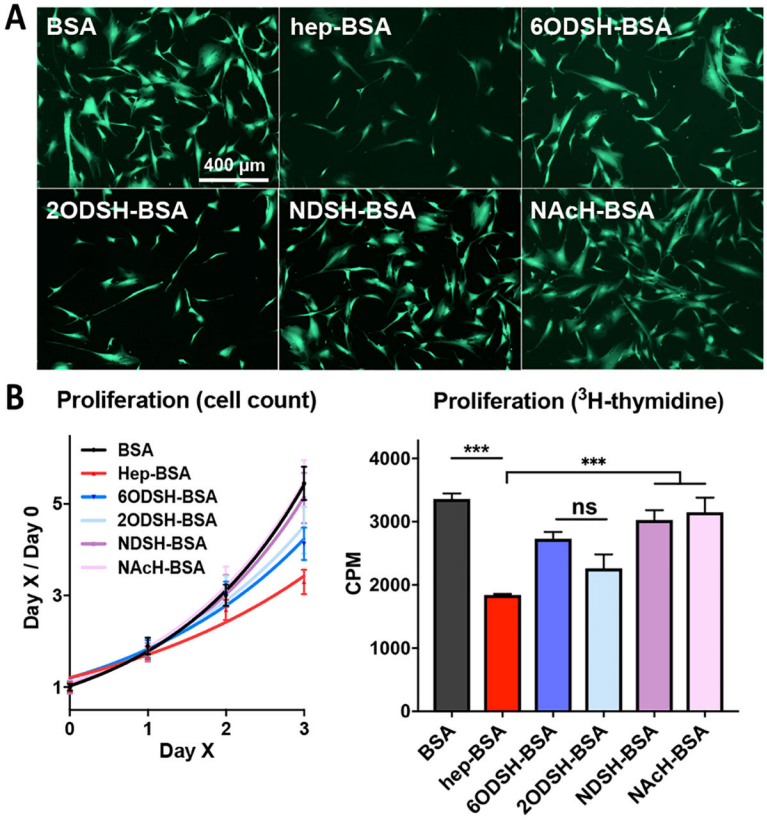

Figure 5.

Immobilized heparinoid–BSA conjugates inhibit hMSC proliferation based on their sulfation pattern and capacity to bind FGF2. (A) Fluorescent micrographs of calcein-stained (1 μM) hMSCs cultured on heparinoid–BSA conjugates (Day 3). (B) Cell counts for hMSCs (Day 0-Day 3). (C) Uptake of ^{3}H-thymidine (0.5 μCi) by hMSCs during Day 3 of culture on immobilized heparinoid–BSA conjugates. (ANOVA, Tukey's multiple comparisons test; $p^{***} < 0.001$)